PROVING SHOCK THICKNESS DECREASES FOR INCREASING MACH NUMBER

By John R. Cipolla, Copyright January 22, 2020

Abstract

Contrary to common belief, shock thickness in supersonic and hypersonic flow is not an unchanging function of Mach number and not simply an infinitely thin discontinuity in the flow field. This discussion proves that shock wave thickness decreases significantly as Mach number increases and is not an absolute and unchanging discontinuity in external and internal flows. To prove that shock thickness decreases significantly with Mach number the specific case of a normal shock wave in the diverging section of a converging-diverging nozzle is considered. This analysis reveals that shock wave thickness becomes significantly smaller as Mach number is increased. Therefore, a shock wave has a finite but very small thickness, dx caused by the "packing" of molecules during the compression process as the shock wave moves through an undisturbed fluid. In addition, fluid density in the region of the shock wave tries to distribute itself evenly during the passage of the shock wave into undisturbed fluid. In this discussion shock thickness is determined as a function of Mach number and fluid viscosity.

Nomenclature

a = Local speed of sound

M = Free stream Mach number

P = Static pressure

R_{gas} = Gas constant

T = Fluid temperature

T_0 = Free stream temperature

V = Fluid velocity

dx = Shock thickness

Greek symbols

μ = Coefficient of viscosity

ρ = Fluid density

ν = Kinematic viscosity (μ/ρ)

γ = Ratio of specific heat

Fluid Dynamics Background Discussion

When an object or fluid disturbance moves so fast that fluid particles cannot move out of the way, the molecular structure of the fluid permits the relative position of the molecules to move closer together or to compress. Thus, as the mean free path of the molecules is shortened, layers of spherical (3D) or planar (2D) disturbances come together to form a shock wave. A pressure build-up or pressure pulse is created which grows larger and larger until it becomes a shock wave resulting in a rise in temperature and pressure. In short, as a disturbance approaches the speed of sound, gas molecules pack closer and closer together until a region of compressed fluid results called a shock wave[1]. A shock wave is actually a wave front of compressed gas molecules with some unique properties. All three-dimensional objects that travel faster than Mach 1 produce shocks and oblique shocks as illustrated in Figure-1 of a projectile traveling at Mach 2.81. The contour plot presented in Figure-1 was generated using the CFD program, AeroCFD[2].

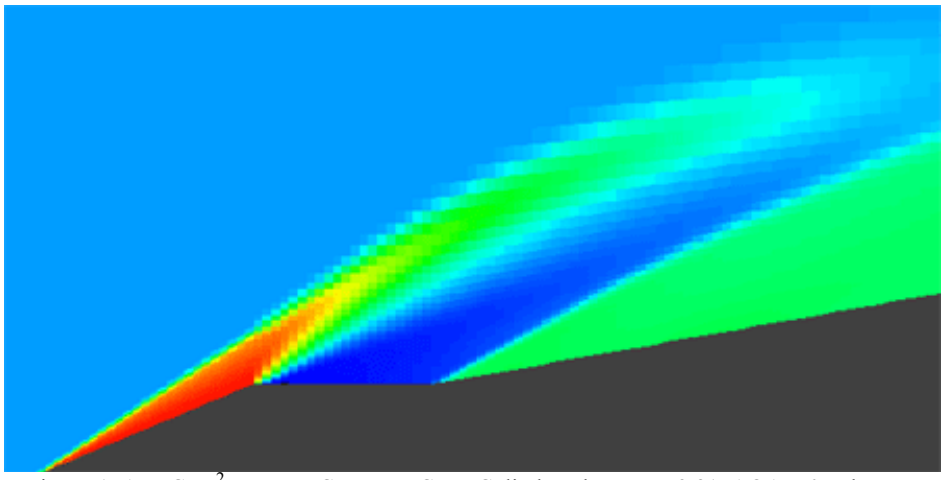

Figure-1, AeroCFD[2] Pressure Contours, Cone-Cylinder-Flare, M = 2.81, AOA = 0.5 degrees

For converging-diverging nozzles[1, 3], fluid flow begins when the exit backpressure, P_e is reduced below the chamber pressure, P_0. If P_e is only slightly less than P_0, the flow throughout the nozzle is subsonic and the pressure profile along the axis would be like curve-A in Figure-1. Reducing P_e increases the mass flow rate through the nozzle. As the flow rate increases, the pressure at the throat decreases until it reaches the critical pressure indicated by curve-B. For the condition represented by curve-B the exit pressure P_e that corresponds to sonic conditions at the throat and subsonic everywhere else can be easily determined using isentropic flow relations. The flow is subsonic everywhere in the nozzle except at the throat and mass flow is the maximum possible for given nozzle and reservoir conditions. Now, suppose the exit pressure is reduced to a value corresponding to curve-F in Figure-1 where no shocks are present in the nozzle. The exit pressure at F is such that the entire expansion is isentropic and the flow is subsonic in the converging portion of the nozzle and supersonic in the diverging section. The value for pressure is simply obtained from the isentropic relationships for Mach number, pressure, temperature and density and represents an optimal nozzle design. The pressure within the nozzle exit cannot be reduced further and when the external pressure is reduced to G the fluid leaving the nozzle changes its pressure through a complicated flow pattern outside the nozzle. Thus, curve-B and curve-F represent the two limiting cases of exit pressure for isentropic flow in such a nozzle. For exit pressures below that at B, a shock wave forms within the diverging part of the nozzle, changing the flow from supersonic to subsonic

and compressing the gas exactly enough to match the nozzle exit conditions. Because of the entropy rise across the shock, the overall flow through the nozzle is **not** isentropic, although the flow on either side of the shock can still be considered isentropic. The lower limit for this kind of flow pattern is given by a shock occurring exactly at the exit of the nozzle as indicated by curve-D. The flow conditions for exit pressures between curve-B and curve-D may be computed with aid of the isentropic relationships and normal shock analysis across the shock. At still lower exit pressures the fluid flow adjusts itself through a series of two-dimensional or three-dimensional shock waves and the average exhaust velocity is generally still supersonic. The nozzle designer must choose an appropriate condition from the previous possibilities for his/her particular application. When the flow leaves the nozzle at supersonic speeds and its pressure exactly equals the surroundings the nozzle is called *correctly expanded* as represented by curve-F. If the exit area of the nozzle is less than the correctly expanded value for a given backpressure, the nozzle is *underexpanded* and the fluid leaving the nozzle has a pressure greater than the surroundings as represented by curve-G. On the other hand, if the exit area of the nozzle is too large, shock waves form within or just outside the nozzle and the flow is called *overexpanded as represented by* curve-E. Establishing the limiting pressure between curve-B and curve-D and comparing them with the specified exit pressure the designer quickly determines the particular mode of operation of any nozzle.

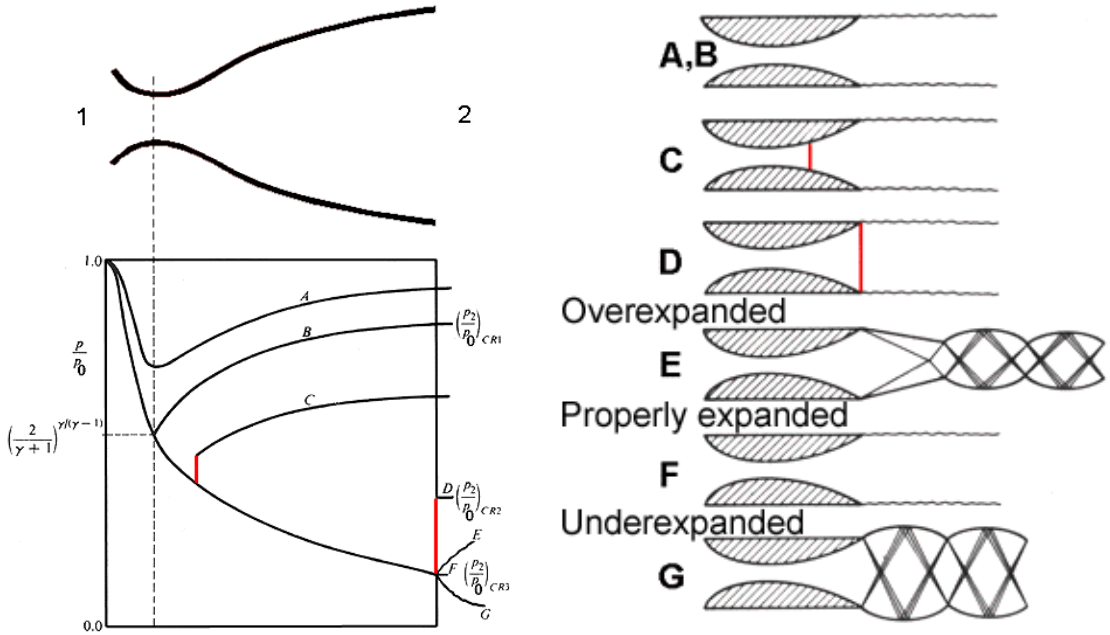

Figure-2 and Figure-3, Nozzle flow conditions depending on Pressure Ratio (P_e/P_0)

Normal Shock Wave Thickness Discussion

To prove that shock thickness decreases significantly with increasing Mach number the specific case of a normal shock wave in the diverging section of a converging-diverging nozzle is considered. Curve-C in Figure-2 represents the condition where a normal shock exists in the diverging portion of the nozzle and is the case used here to compute normal shock thickness as a function of Mach number. Some engineers and Computational Fluid Dynamics[4] (CFD) researchers incorrectly define a shock wave as an infinitely thin discontinuity in the flow. This misconception is probably due to the fact that CFD codes rarely attempt to mesh the region within a shock wave because of the huge computational resources required. However, a shock wave is not discontinuous, i.e. a shock wave is not

infinitely thin, because a shock wave has a finite thickness where fluid properties vary continuously across the region defined within the shock wave. Upstream of a normal shock the flow is supersonic, whereas downstream of a normal shock the flow is always subsonic. In addition, upstream and downstream of a shock wave the flow is isentropic but the flow is not isentropic in a region defined by the shock wave. The flow is not isentropic in a shock wave because friction or shear stress causes the flow to be internally irreversible. Within a shock wave, internal irreversibility (losses) due to friction cause the entropy, ds to be greater than 0.0. Whereas, before and after a shock wave ds = 0.0.

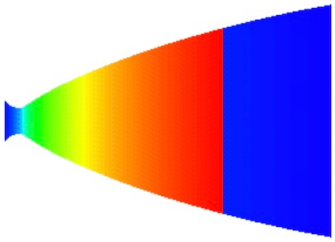

Figure-4, Backpressure (P_e/P_0) that causes a normal shock in the diverging part of the nozzle, curve-C

Normal Shock Wave Thickness Analysis

This analysis reveals that shock wave thickness[5] becomes significantly smaller as Mach number is increased. Therefore, a shock wave has a finite but very small thickness, dx caused by the "packing" of molecules during the compression process as the shock wave moves through an undisturbed fluid. The density of the fluid in the region of a shock tries to distribute itself evenly during the passage of the shock wave into undisturbed fluid. The equations that follow determine shock wave thickness as a function of Mach number before the shock, M_1 and fluid viscosity, ν.

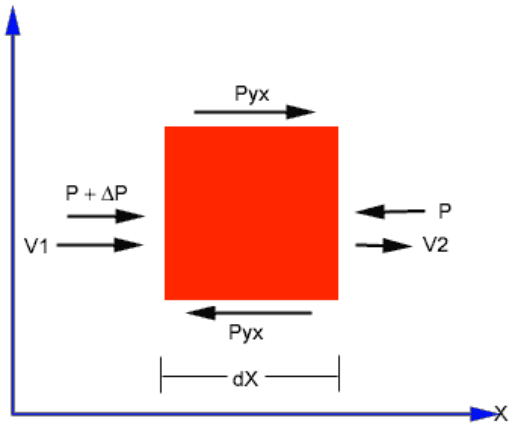

Figure-5, Control volume around a normal shock wave

Figure-5 displays the control volume around a shock wave that assumes the fluid is in motion past a stationary shock. In addition, the applied shear stress, P_{yx} is proportional to the velocity gradient in the x-direction for common linear fluids like air. The equation for shear stress[1, 3] acting on the shock control volume is the following.

$$P_{yx} = \mu \frac{du}{dx}. \tag{1}$$

Assume that for the control volume displayed in Figure-5, the shear stress, P_{yx} acting within the shock is approximately equal to the normal stress[1, 3], ΔP acting on the shock.

$$P_{yx} \approx \Delta P = P_2 - P_1. \tag{2}$$

After Substituting Equation 2 into Equation 1 the following relationship is achieved.

$$P_2 - P_1 = \frac{\mu(V_1 - V_2)}{dx}. \tag{3}$$

Define the continuity equation[1, 3] for fluid mechanics.

$$\rho_1 V_1 = \rho_2 V_2. \tag{4}$$

Define the x-momentum equation[1, 3] for fluid mechanics.

$$P_1 - P_2 = \rho_2 {V_2}^2 - \rho_1 {V_1}^2. \tag{5}$$

Determine shock pressure change using the continuity and x-momentum equations.

$$P_2 - P_1 = \rho {V_1}^2 \left(1 - \frac{V_2}{V_1}\right). \tag{6}$$

After Substituting Equation 6 into Equation 3 the shock thickness, dx is.

$$dx = \frac{\mu}{\rho}\left[\frac{1 - \frac{V_2}{V_1}}{V_1\left(1 - \frac{V_2}{V_1}\right)}\right]. \tag{7}$$

Then, after simplification, Equation 7 becomes, where $\nu = \frac{\mu}{\rho}$.

$$dx = \frac{\nu}{V_1}. \tag{8}$$

The local speed of sound[1, 3] before the shock wave is the following.

$$a_1 = \sqrt{\gamma R_{gas} T_1}. \tag{9}$$

Mach number[1, 3] before the shock when fluid velocity is known are.

$$M_1 = \frac{V_1}{a_1}. \text{ Where } V_1 = a_1 M_1. \tag{10}$$

Finally, shock wave thickness, dx in terms of initial Mach number and viscosity is.

$$dx = \frac{\nu}{a_1 M_1}. \tag{11}$$

Numerical Algorithm For Shock Wave Thickness

Fluid properties and numerical constants before the shock wave are the following.

$T_0 = 288.15\ K$ $\quad \gamma = 1.4$ $\quad \nu = 1.4607\ x\ 10^{-5}\ \frac{m^2}{sec}$ $\quad R_{gas} = 287\ \frac{m^2}{sec^2 K}$

$I_{max} = 100$ $\quad M_{max} = 20$ $\quad M_{min} = 1$

Generate array of Mach number values before the stationary shock wave.

$$M_i = M_{min} + (M_{max} - M_{min})\frac{i-1}{I_{max}-1}. \tag{12}$$

Generate array of temperature[1] values before shock wave as a function of Mach number.

$$T_i = T_0\left(1 + \frac{\gamma - 1}{2} {M_i}^2\right)^{-1}. \tag{13}$$

Generate array of speed of sound[1] values before shock as a function of temperature.

$$a_i = \sqrt{\gamma R_{gas} T_i}. \tag{14}$$

Finally, determine shock thickness, dx as a function of Mach number, M.

$$dx = \frac{\nu}{a_i M_i}. \tag{15}$$

Normal Shock Thickness Example
Shock thickness decreases with increasing Mach number

The following example uses Equation 15 to determine normal shock thickness in the diverging section of a converging-diverging nozzle when free stream velocity is Mach 2.81. The Standard Atmospheric value[6] for air temperature, T_0 at sea level is 15 C and kinematic viscosity, ν for air is 1.4607 x 10^{-5} m^2/sec. In figure-6 the normal shock thickness is plotted as a function of Mach number. For this example at Mach 2.81 the shock wave thickness is determined from Equation 15 to be 2.453 x 10^{-5} mm and is represented as a **blue dot** in the dx verses Mach number plot in Figure-6. Please note that in Figure-6 shock wave thickness as a function of Mach number is normalized by shock wave thickness at Mach 1. Figure-6 illustrates that normal shock wave thickness; dx varies from 4.703 x 10^{-5} mm at Mach 1 to 1.932 x 10^{-5} mm at Mach 20. This analysis proves that shock wave thickness decreases with increasing Mach number representing a 41.1 percent decrease in shock thickness from Mach 1 to Mach 20.

Figure-6, Normal shock thickness as a function of Mach number from Mach 1 to Mach 20

History of the Shock Thickness Results Presented Here

This paper presents results and basic principals that were rejected during a presentation to leadership of the CFD Section of the Munitions Directorate at the Air Force Research Laboratory (AFRL) that proved shock thickness decreases for increasing Mach number.

Beginning June 1989 John Cipolla was the first Eglin Air Force Base engineer to develop the capability to simulate holographic interference flow fields and **shock wave patterns** from **C**omputational **F**luid **D**ynamics solutions and then successfully compare these flow patterns with experimentally obtained interferograms. John Cipolla's work in the area of interferometric analyses for predicting shock wave patterns from CFD results was documented in his report, ***Computational and Experimental Interferometric Analysis of a Cone-Cylinder-Flare Body***[7] and was presented in November 1989 after six months of intense work. Figure-7 presents a theoretical interferogram[7] for supersonic flow past a body at Mach 2.81 that was a point of discussion. During the staff briefing to several USAF AFRL/MN personnel, John Cipolla was about to discuss the fluid dynamics

mechanism that causes **shock thickness** to decrease with increasing Mach number. However, Dr. Davy Belk and other AFRL research personnel disagreed and insisted without proof that shock wave thickness could not possibly decrease or even change with increasing Mach number. However, Reference 5 independently demonstrates that shock wave thickness does indeed decrease with increasing Mach number. This paper, which proves shock wave thickness decreases with increasing Mach number, is a long overdue response to the USAF AFRL/MN researchers.

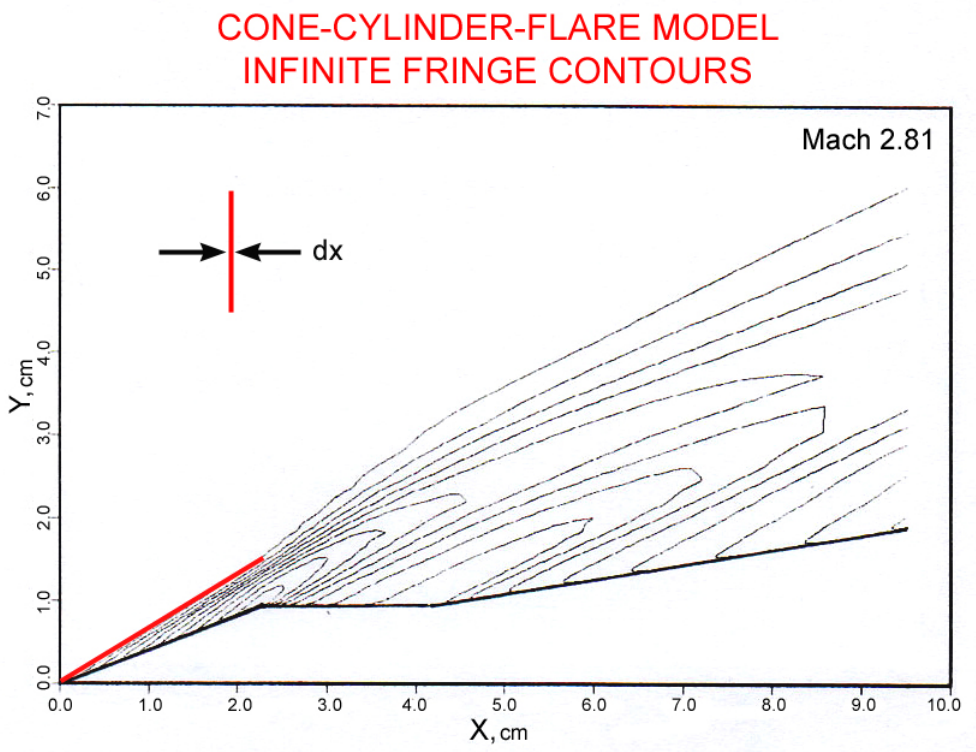

Figure-7, Theoretical Interferogram generated in the Aeroballistic Tunnel at Eglin AFB

REFERENCES

[1]F. M. White, *Fluid Mechanics*, (McGraw-Hill, New York, 2010)

[2]John Cipolla, AeroCFD®, 3D and 2D Computational Fluid Dynamics (CFD) code, AeroRocket.com

[3]Sabersky, Acosta, Hauptmann, *Fluid Flow-2nd Edition* (The Macmillan Company)

[4]John D. Anderson, *Computational Fluid Dynamics: the basics with applications* (McGraw-Hill, 1995)

[5]Robert A. Granger, *Fluid Mechanics*, p.845 to 846 (Dover Publications, Inc., 1985, 1995)

[6]D. Halliday, R. Resnick, *Fundamentals of Physics-7th Edition* (John Wiley & Sons, New Jersey, 2005)

[7]John Cipolla, "Computational and Experimental Interferometric Analysis of a Cone-Cylinder-Flare Body", Air Force Armament Laboratory, Eglin AFB, (1989, 2015), https://vixra.org/pdf/1504.0185v1.pdf